Ecosystems (2026) 29:60
https://doi.org/10.1007/s10021-026-01084-w

ORIGINAL ARTICLE

Fungal Community Composition Better Explains Variation in Wood Decomposition than Fungal Biomass in a Northern Temperate Deciduous Forest

Christian Hettwer,[1]* Peter Avis,[2] Andrew Ouimette,[3] Karl Bishop,[4] Colby Bosley-Smith,[5] Heather Richard,[2] Rose Z. Abramoff,[5] Anthony W. D'Amato,[6] and Shawn Fraver[5]

[1]*Department of the Geophysical Sciences, University of Chicago, Chicago, Illinois 60637, USA;* [2]*School of Biology and Ecology, University of Maine, Orono, Maine 04469, USA;* [3]*USDA Forest Service, Northern Research Station, Durham, New Hampshire 03825, USA;* [4]*Department of Chemistry, University of Maine, Orono, Maine 04469, USA;* [5]*School of Forest Resources, University of Maine, Orono, Maine 04469, USA;* [6]*Rubenstein School of Environment and Natural Resources, University of Vermont, Burlington, Vermont 05405, USA*

Abstract

Despite growing scientific evidence of the important role that wood-decomposing fungi serve in ecosystem function, we know little about how fungal community dynamics relate to decomposition outcomes. We deployed 42 standardized (same dimensions and source) wood stakes from sugar maple (*Acer saccharum*) and white ash (*Fraxinus americana*) on the forest floor of a northern US hardwood forest. After four years, we collected the stakes for analysis of fungal biomass (via ergosterol), community composition (DNA sequencing), and nutrient concentrations. We found large variability in mass loss (9–95% for sugar maple, 4–36% for white ash), with sugar maple stakes showing much greater mass loss than white ash. Fungal community composition, summarized by PCoA axes, was a significant predictor of mass loss for both wood species, with fungal biomass explaining additional variability in some models. As expected, lower C/nutrient ratios (higher fraction of initial nutrient remaining, X/X_0) were associated with greater mass loss. We found consistently stronger correlations of fungal community composition, compared to fungal biomass, with C/nutrient ratios in sugar maple stakes. White ash stakes showed consistent correlations of both fungal community composition and fungal biomass with C/nutrient

Received 13 January 2026; accepted 7 June 2026

Supplementary Information: The online version contains supplementary material available at https://doi.org/10.1007/s10021-026-01084-w.

Author Contributions Christian Hettwer: Conceptualization, Methodology, Data Collection, Analysis, Writing, Visualization, Editing. Peter Avis: Conceptualization, Methodology, Data Collection, Analysis, Writing, Editing. Andrew Ouimette: Conceptualization, Analysis, Visualization, Editing. Karl Bishop: Methodology, Data Collection. Colby Bosley-Smith: Methodology, Data Collection, Editing. Heather Richard: Methodology, Data Collection. Rose Abramoff: Conceptualization, Editing. Anthony D'Amato: Conceptualization, Data Collection, Editing. Shawn Fraver: Conceptualization, Methodology, Data Collection, Analysis, Writing, Visualization, Editing.

*Corresponding author; e-mail: hettwer@uchicago.edu

Published online: 30 June 2026

ratios. Lastly, redundancy and cluster analyses showed that fungal communities clustered into taxonomically distinct groups that also corresponded to differences in mass loss. Together, our results suggest that communities with low biomass but efficient decomposers are associated with faster decomposition, while communities with high biomass but less efficient decomposers may not necessarily correlate with high mass loss. Our results suggest that wood decomposition and forest ecosystem models could be improved by including fungal community composition and total fungal biomass.

Key words: wood decomposition; wood-decay fungi; ecosystem ecology; carbon; nutrient cycling; fungal community; ergosterol; forest ecology.

Introduction

Wood decomposition is a fundamental process in terrestrial ecosystems, influencing carbon cycling and nutrient turnover at both local and global scales. The decomposition of deadwood, which can represent as much as 30% of a forest's total biomass, releases carbon dioxide (CO_2) to the atmosphere through fungal respiration (Harmon and others 1986; Woodall and others 2008; Pan and others 2011). Nutrient cycling during decomposition is a dynamic process, with fungal decomposers initially immobilizing or retaining nutrients before gradually mobilizing otherwise inaccessible pools. Through this shifting balance, they enhance soil fertility, support plant growth, and sustain the long-term productivity and resilience of forest ecosystems (Johnson and others 2014). While decomposition is generally well studied, the factors regulating variability in decay rates remain less clear, with evidence suggesting that climate alone may be a poor predictor of wood decomposition (Bradford and others 2014).

Fungal biomass, often quantified via ergosterol, is a measurable link between decomposition activity and substrate nutrient composition. As the principal agents of lignocellulose breakdown, fungi invest resources into hyphal growth and enzyme production, and the resulting fungal biomass reflects the intensity of decomposer activity (Seibold and others 2022; Micó and others 2024). Fungal proliferation is strongly constrained by nutrient availability, with limited nitrogen (N), phosphorous (P), or other essential elements reducing growth rates and enzymatic capacity, thereby modulating decomposition outcomes (Sterner and Elser 2002). While studies have linked fungal biomass and substrate physiochemistry, it remains unclear how fungal biomass scales with C/nutrient ratios in driving decomposition and to what extent this relationship explains variability in mass loss (Lustenhouwer and others 2020). Elucidating these relationships is critical for improving mechanistic models of forest-scale decomposition processes and carbon sequestration.

The composition of fungal communities can influence decay trajectories as decomposer taxa vary in nutrient requirements and decay strategies (Fukami and others 2010; Maynard and others 2018; Viotti and others 2021; Yang and others 2024). Fungal functional groups (white rot, brown rot, and soft rot) differ in their enzymatic capabilities and substrate preferences, producing distinct patterns of wood breakdown (Boddy 2001; Lustenhouwer and others 2020; Schilling and others 2020). These functional differences not only shape the rate and extent of decomposition but also influence nutrient cycling within the substrate. Empirical studies indicate that initial fungal colonizers significantly affect mass loss outcome and community trajectory in wood decomposition (Lindner and others 2011). Much of the variance in fungal community composition, and in turn wood decomposition, is explained by wood species and wood physiochemical properties (e.g., N content) (Purahong and others 2018; Yang and others 2024). Other studies have shown that fungal communities shift in response to nutrient availability, with certain taxa dominating under specific C/nutrient conditions (van der Wal and others 2015; Fukasawa 2021). Furthermore, fungal community richness is inversely related to decay rates, likely due to competition for resources (Perreault and others 2023). However, despite this evidence, few studies explicitly link fungal community composition to patterns of wood mass loss and nutrient stoichiometry, representing a key gap in our understanding of decomposition ecology.

Nutrient stoichiometry, particularly when carbon-to-nutrient ratios (C/nutrient) are high, is a central constraint on decomposition rates because wood is typically nutrient poor (Laiho and Prescott 1999, 2004; Manzoni and others 2010). Deadwood contains high amounts of structural carbon but very low concentrations of N and P, producing C/N and C/P ratios that limit decomposer metabolism (Boddy and Watkinson 1995). Studies of coarse woody material show that nutrient concentrations generally increase with decay stage, as wood loses carbon mass and becomes relatively enriched in N

and P, although absolute nutrient contents may decline depending on the balance of leaching and external inputs (Harmon and others 1994; Holub and others 2001; Romero and others 2005; Klockow and others 2014). Such stoichiometric imbalances influence fungal growth efficiency, as microbes must expend additional energy to acquire limiting nutrients, constraining enzyme production and slowing decomposition (Hobbie and Vitousek 2000; Craine and others 2007; Wu and others 2021). Despite strong evidence from soil and leaf litter that nutrient stoichiometry regulates decomposition rates, the specific role of nutrient availability in governing fungal community dynamics remains poorly resolved. In particular, while the roles of N and P have been relatively well studied, the influence of other elements (e.g., potassium (K), calcium (Ca), magnesium (Mg), micronutrients) is far less understood (Dalling and others 2024). While minor elements zinc (Zn), boron (B), copper (Cu), and iron (Fe) are known to accumulate by some wood-decay fungi, specifically white rot, their association with community assembly and decomposition outcomes are poorly constrained (Krzesłowska and others 2025).

Here, we examined how fungal biomass and community composition correspond to decomposition outcomes of standardized wood stakes. With an overarching goal of understanding fungal and biochemical dynamics in wood decomposition, our objectives were the following: (1) to determine the importance of fungal biomass and community composition in explaining variation in mass loss and (2) to assess how fungal biomass and community composition relate to nutrient stoichiometry.

Methods

Study Site and Sample Preparation

The study was conducted in a mature, closed-canopy northern hardwood forest near Corinth, Vermont, USA (44° 2′ N and 72° 17′ W). The site is dominated by sugar maple (*Acer saccharum*) and white ash (*Fraxinus americana*), with yellow birch (*Betula alleghaniensis*) and American beech (*Fagus grandifolia*) present in lesser amounts (Legge and others 2025). This site supports a range of recent silvicultural trials, including three unharvested control blocks (each ca. 6 ha, separated by 550 m on average), the focus of the current study. Each control block included seven 11.3 m radius plots established to characterize tree overstory structure and composition. Mean annual temperature at the site is 5.3°C, with annual precipitation of 1139 mm based on climate data from 1991 to 2020 (PRISM Group 2024). Plot-level environmental conditions were not measured in this study.

To meet our objectives related to wood decomposition, we manufactured decay stakes (n = 24 per species) to be deployed in the field for later collection. Three stakes of each species were undeployed, thus serving as controls. This set of stakes (n = 48 total) was used for all analyses. Stakes were manufactured from rough-sawn, furniture-grade planks of sugar maple and white ash (the site's two dominant tree species) purchased at a local mill. Only bark-free sapwood was used, based on wood color. In our university shop, planks were rip-sawn and planed to 2.5 × 2.5 cm before being cut to lengths of 20 cm. As they were being cut to length, the order and unique numbering of the stakes was randomized to ensure that stakes ultimately placed on individual field plots had not arisen from the same plank. Stakes were oven dried (75°C for 8 days), weighed while dry, and deployed on the forest floor in May 2020. Decay stakes were placed in groups of two (one of each species) immediately outside the plot border, maintaining 20 cm between stakes. Stake placement around the plot border was selected by a random azimuth from plot center. Stakes were held in place with landscaping staples and were collected in September of 2024 (deployed for four full growing seasons).

After collection, samples were maintained at 4°C in darkness for three days before DNA extraction and one month for ergosterol analysis (Lauber and others 2010). Stakes were then cleaned (to remove soil and leaves) and drilled to obtain wood shavings, which were used for ergosterol content, nutrient content, and DNA sequencing. The shavings were then prepared for the various analyses (below), and the stakes were dried for mass loss calculations. The stake remains were then reweighed for mass loss (%), accounting for masses of stakes used in subsequent analyses.

Fungal Biomass via Ergosterol Content

Ergosterol, an important compound for fungal development and growth found in the cell membrane of most wood-decay fungi and routinely quantified as a proxy for fungal biomass, was analyzed according to methods outlined by Newell and others (1988) and Micó and others (2024). In the laboratory, wood shavings were collected by first removing the exterior layer of wood with a sterile razor blade at three locations (approx. 2.5 cm from each end and in the middle of the

stake) and drilled using a sterile drill bit. Shavings from each stake were composited then milled into a homogenous, fine powder (1 g) with a ball mill and stored overnight in 7.5 mL of methanol at 4°C in darkness. The wood powder in methanol was placed in a dry bath at 65°C for 2 h, with shaking every 30 min, followed by a cool bath for 5 min. 1 mL of saponification fluid (0.04 g/mL KOH in ethanol) was added to each sample, followed by 30 min in the dry bath and 5 min in the cool bath. The saponified samples were centrifuged at 4000 rpm for 5 min. We then decanted and rinsed with 1 mL of methanol thrice, pooling decants. Distilled water (0.5 mL) was added to the pooled supernatants to develop a density barrier, which allowed for pentane (1 mL) extraction of ergosterol. After evaporating pentane overnight, the extraction residue was diluted in 1 mL of methanol, filtered with 0.2 µm, and injected into an Agilent Technologies HPLC system with a C18 column. At a flow rate of 1.5 mL min^{-1} of the methanol mobile phase and a detector wavelength of 282 nm, ergosterol was detected approximately 1.3 min after injection. Determination of fungal biomass from ergosterol content followed the conversion factor of 3.8 mg of ergosterol per gram of fungus, assuming a carbon concentration of 47.2% in fungal biomass (Koide and Malcolm 2009; Baldrian and others 2013).

Nutrient Quantification

Nutrient concentrations in wood samples (n = 24 per species) were measured to assess functional relationships with mass loss. Macronutrients measured included carbon (C), phosphorous (P), nitrogen (N), potassium (K), calcium (Ca), and magnesium (Mg). Micronutrients measured included boron (B), copper (Cu), iron (Fe), manganese (Mn), aluminum (Al), and zinc (Zn). Milled and homogenized samples were analyzed at the Analytical Laboratory at the University of Maine. Fraction of initial nutrient remaining (denoted X/X_0) for each nutrient was calculated as final absolute nutrient mass in decayed stakes divided by initial absolute nutrient mass in undeployed controls. C/nutrient ratios were calculated as C concentration (%) divided by the nutrient (e.g., N, P, K) concentration (%).

DNA Sequencing and Bioinformatics

Samples for fungal DNA metabarcoding were collected from decay stakes (n = 24 per species) following a modified version of the approaches described in Purahong and others (2014) and Runnel and others (2021). After field collection, each decay stake was lightly cleaned of larger debris and a thin layer of the outermost portion of the stake was removed by razor blade to expose the inner wood. Wood tissue was then removed using a sterilized 3 mm (1/8-inch) bit drilled into the decay stake at three locations adjacent to the same locations in which samples were taken for ergosterol. Extracted tissue was placed into 4 mL centrifuge tubes and frozen at −20°C. In cases where decay stakes were extremely wet, punky, and/or difficult to sample in this way, sterilized forceps were used to remove tissue.

Each sample was separately submerged in liquid nitrogen and then pulverized to a flour-like texture using a mortar and pestle. The DNA from approximately 100 mg of each pulverized sample was extracted using a kit-based approach (Thermo Scientific GeneJET Plant Genomic DNA Purification Kit). The DNA concentration of each extract was determined fluorometrically (Qubit). Subsequently, PCR and metabarcoding of the fungal ITS2 region was conducted following a modified version of Avis and others (2025). Briefly, this protocol uses the ITS3_KYO2 and ITS4_KYO3 primer set (Toju and others 2012; Morvan and others 2020) flanked by Illumina Nextera adapters. We used BioRad iTaq SuperMix supplemented with BSA and the following amplification conditions: initial denaturation of 95°C for 3 min followed by 35 cycles of 94°C for 30 s, 53°C for 45 s, 72°C for 1 min and a final elongation at 72°C for 10 min. Amplicon metabarcoding was then conducted on the Illumina MiSeq platform and the NExtera XT DNA Library Preparation process at RI INBRE Molecular Informatics Core at the University of Rhode Island.

A bioinformatic pipeline involved FAST QC for quality control of sequence reads, cutadapt for primer trimming, filtering, chimera removal, and dereplication. Amplicon sequence variants (ASVs) were determined using DADA2, and taxonomy was assigned using UNITE version 10.0 (Abarenkov and others 2024). Consistent with findings from Buness and others (2026) and Kubartová and others (2015), single-endpoint metabarcoding after four years of decay provides a community-level snapshot that captures both living and recently dead fungal mycelium, alongside a broad set of early- and mid-successional taxa. This enables linkage of fungal community composition to observed mass loss while integrating signals from taxa contributing to decomposition trajectories over time. However, because our methodology cannot partition active versus recently dead fungal biomass (and

may also detect spores and relic DNA), this snapshot does not fully resolve successional dynamics or isolate the actively decomposing community at the time of sampling.

Sequence data were then processed and organized using the *phyloseq* package in R (McMurdie and Holmes 2013), where ASV abundance tables, representative sequences, taxonomic assignments, and sample metadata were combined into a unified phyloseq object. 108 unique ASVs were measured and included in analyses. We then conducted a principal coordinate analysis (PCoA) of generalized UniFrac distances based on ASV similarity using the *ape* package in R (Paradis and others 2004), which inherently accounts for differences in library size and compositional structure. Principal coordinates analysis (PCoA) was then performed on the resulting distance matrix. Doing so allowed us to assess the similarity in fungal community among samples and to generate coordinate axes (PCoA1 and PCoA2) to be utilized as potential predictors of mass loss. Statistical analyses were done separately for the two stake wood species. All data processing and statistics were conducted in R (R Core Team 2025) using RStudio (Posit Team 2025).

Data Analysis

To determine the important fungal predictors of mass loss, we conducted multiple linear regressions, where mass loss (%) was the response and fungal biomass (mg/g) and PCoA coordinates were predictors. Using the ''lme'' function in the *nlme* package (Pinheiro and others 2025), where blocks were treated as random effects, we tested various combinations of important predictors, both interactive and additive, using a deductive approach of omitting variables that were not statistically significant based on p values ($\alpha = 0.05$). We then compared models based on corrected Akaike's information criterion (AICc), allowing us to assess which model forms were best supported by the data. All predictor variables were standardized (mean = 0, standard deviation = 1), using the ''scale'' function in base R, before model fitting to assess effect sizes among predictors having different units.

To identify how fungal community and fungal biomass influenced nutrient stoichiometry outcomes, we conducted two analyses. First, we calculated Pearson correlation coefficients between fungal variables (biomass, PCoA1, or PCoA2) and X/X_0 for each nutrient. Significance of Pearson correlations was determined via p values ($\alpha = 0.05$). Second, we conducted a Redundancy Analysis (RDA) using the ''rda'' function in the *vegan* package (Oksanen and others 2025). The multivariate response included X/X_0 of each nutrient and the predictors were the first two axes (PCoA1 and PCoA2) from the PCoA, as well as fungal biomass. Significance was assessed via 999 permutations. We binned samples for each wood species by low, intermediate, and high mass loss (roughly equal binning based on mass loss distribution) for spatial visualization of the model results. This approach allowed us to assess the extent to which variation in fungal community structure and biomass explained nutrient variation across a mass loss gradient.

To evaluate differences in nutrient outcomes among fungal taxa that decompose wood at different rates, we conducted a cluster analysis based on community structure. We conducted hierarchical clustering using Ward's method on Euclidean distances of the ordination scores (PCoA axes), using the *vegan* package. The optimal number of clusters ($k = 3$) was chosen based on ecological interpretability along with visual inspection of dendrogram outputs (Supplemental Figure A). We used one-way ANOVAs to assess statistical difference in mass loss (%) and C/nutrient outcomes among clusters. To identify dominant taxa within each community cluster, ASV abundance data were merged with taxonomy at the species-level using the ''psmelt'' function in the *phyloseq* package (Supplemental Table A, Supplemental Figure A). The most abundant fungal taxa per cluster were determined by aggregating taxonomic relative abundances across samples.

Results

The dominant fungal species were *Phanerochaete laevis*, *Steccherinum fimbriatum*, and *Crepidotus occidentalis* for sugar maple wood, and *Pholiota lenta*, *P. laevis*, and *S. fimbriatum* for white ash wood (Figure 1). *P. laevis* and *S. fimbriatum*, the common dominant fungal species between the two wood species, are associated with white rot, while *P. lenta* and *C. occidentalis* are associated with brown rot (Schmidt 2006).

Mass loss varied substantially after four growing seasons, with sugar maple stakes ranging from 9 to 95% mass loss, and white ash from 4 to 36% (Supplemental Figure B). Overall maple had greater percentage mass loss (mean = 35.8) than white ash (13.4). While top-performing linear regressions for predicting mass loss differed by wood species, the top models (based on AICc scores) for both species included a PCoA term and

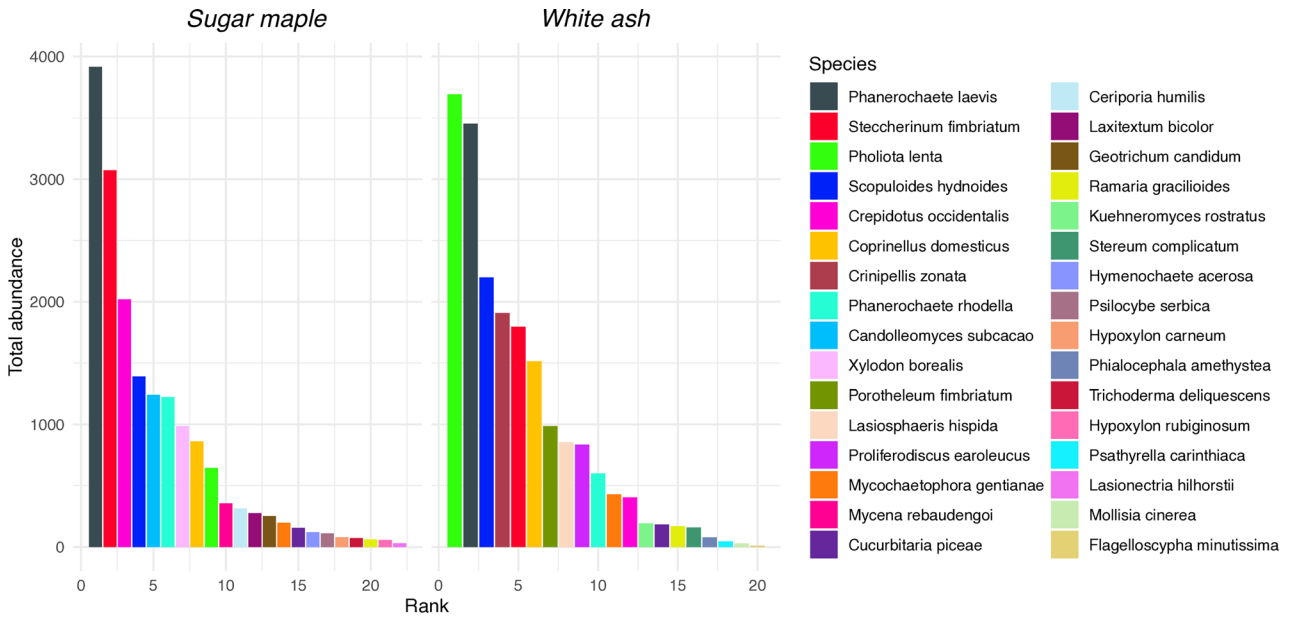

Figure 1. Rank abundance plot showing all taxonomically identified fungal species for sugar maple (left) and white ash (right) samples. Total abundance is based on sequence reads.

Table 1. Top Three Linear Models for Predicting Mass Loss, Ranked by Increasing AICc Scores

Wood species	Model predictors	Effect size, term			*k*	AICc	ΔAICc	AICc wt	R^2
		1	2	3					
Sugar maple	PCoA1* + fbiomass	−15.3	6.4		2	173.7	0.0	0.47	0.48
	PCoA1*	−14.3			1	174.0	0.3	0.41	0.41
	PCoA1* + PCoA2	−14.1	3.2		2	176.4	2.7	0.12	0.40
White ash	PCoA2* + fbiomass*	7.4	3.6		2	115.5	0.0	0.81	0.77
	PCoA2* + fbiomass* + PCoA1	7.7	4.8	1.5	3	118.9	3.4	0.15	0.76
	PCoA2* × PCoA1	8.8	−0.9	−2.7**	3	121.7	6.2	0.04	0.72

ΔAIC is the difference in AICc between the model and the top-performing model (lowest AICc score). AICc wt. is the relative likelihood of each model being the best model, where k represents the number of estimated parameters, R^2 represents the adjusted coefficient of determination, and effect sizes (β coefficients) are for standardized predictors. PCoA variables indicate fungal community composition, and fbiomass indicates fungal biomass.
**Indicates $p < 0.05$.*
***Indicates interaction term.*

fungal biomass as predictors (Table 1). For sugar maple stakes, PCoA1 was present in all top models, with additional variance explained by fungal biomass or PCoA2 as additive terms. PCoA1 was the only significant ($p < 0.05$) predictor across the top three sugar maple models. For white ash stakes, PCoA2 was present in all top models, with additional variance explained by fungal biomass and PCoA1 in two models. One white ash model included a significant interaction between PCoA2 and PCoA1, where simultaneous increases in predictors amplified the effect on the response. In assessing single-predictor linear regressions, PCoA1 was once again the only significant predictor of mass loss for sugar maple stakes (Figure 2). For white ash, fungal biomass, PCoA1, and PCoA2 were significant predictors, with PCoA2 showing the highest R^2 value (0.68). For both wood species, increases in PCoA1 were associated with decreases in mass loss (based on simple linear regressions), while increases in PCoA2 were associated with increases in mass loss (although not statistically significant for sugar maple).

For sugar maple, the wood species with relatively higher variability in decomposition rates, mass loss was weakly correlated with X/X_0 for each nutrient (Figure 3a). White ash, on the other hand, showed consistently strong and positive correlations of mass loss with X/X_0 for all nutrients (except K, Cu, and B), indicating that higher mass loss corre-

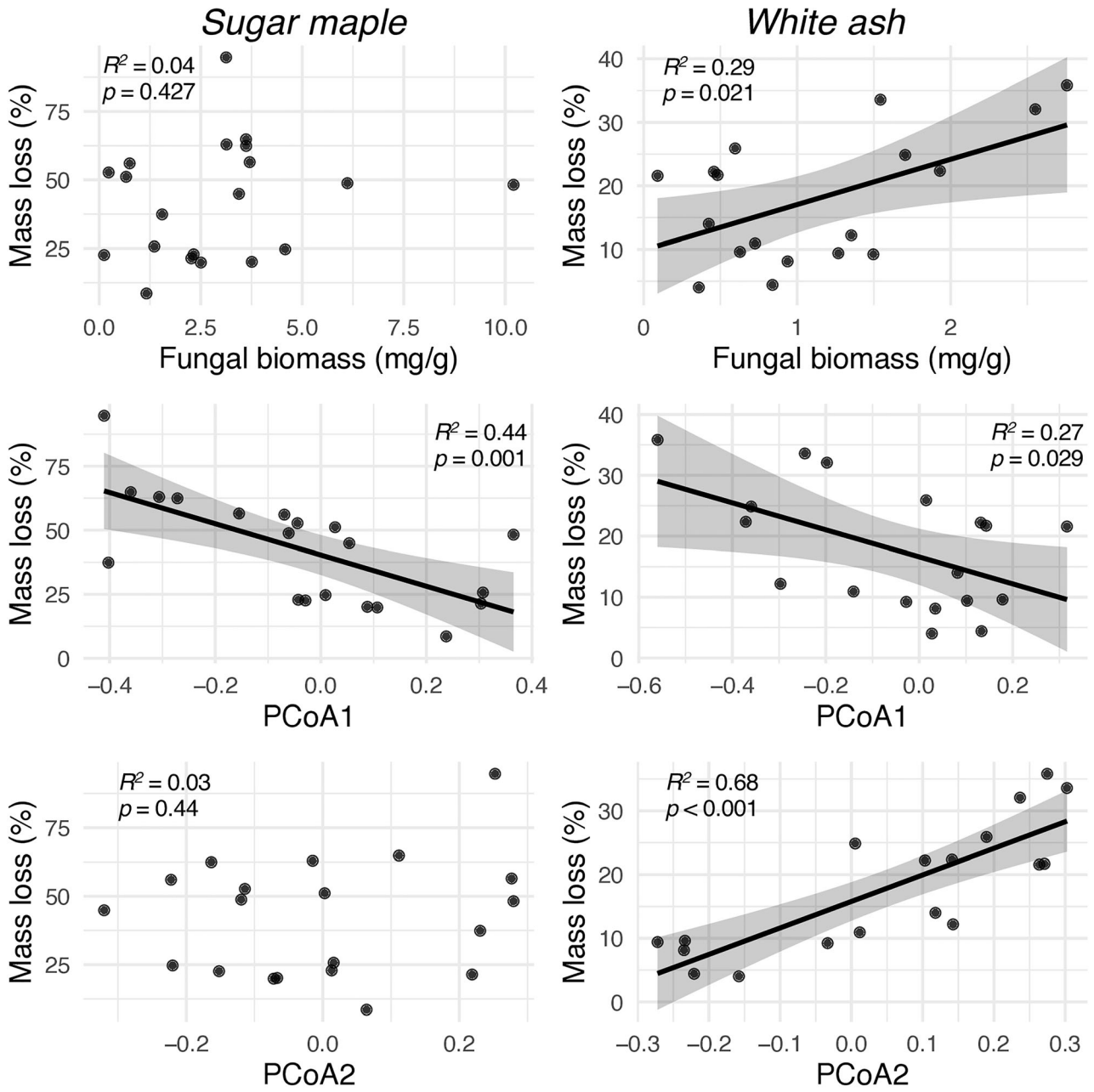

Figure 2. Mass loss (%) as a function of fungal predictors, where PCoA axes represent community composition. Linear regressions (solid line) and 95% confidence intervals (shaded area) are fit for significant regressions ($p < 0.05$).

sponded to higher nutrient concentrations (Supplemental Figure C). Fungal biomass showed similarly weak and inconsistent correlations with nutrient X/X_0 in sugar maple stakes, whereas white ash stakes exhibited consistently stronger positive correlations between fungal biomass and X/X_0. For sugar maple, PCoA1 was correlated with every X/X_0 except Fe and Al. For white ash, either PCoA1 or PCoA2 was correlated with each nutrient X/X_0 (except Cu).

Across wood species, mass loss was strongly and negatively correlated with all C/nutrient ratios (Figure 3b), indicating that higher mass loss corresponded to reduced carbon content and higher relative nutrient concentrations (except K in sugar maple and K and Cu in white ash). Fungal biomass showed only weak negative correlations with C/N and C/P in sugar maple, whereas white ash stakes exhibited consistently stronger negative correlations between fungal biomass and C/nutrient ra-

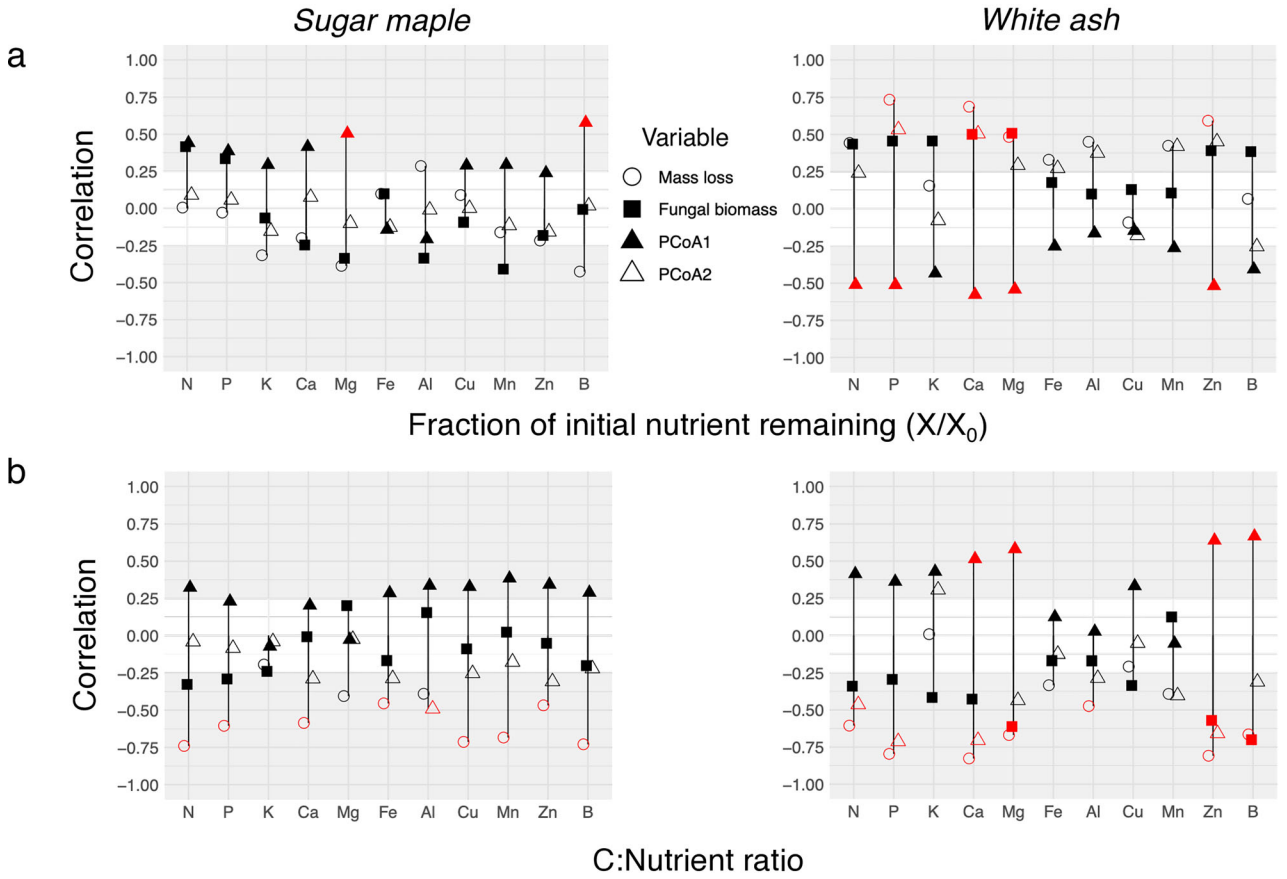

Figure 3. Correlation strengths of (**a**) fraction of initial nutrient remaining (calculated as final absolute nutrient mass divided by initial nutrient mass) and (**b**) C/nutrient ratios with mass loss, fungal biomass, PCoA1, and PCoA2. Black points indicate correlations with $p > 0.05$, and red indicates $p < 0.05$. Shaded areas on the plots indicate correlations greater than 0.25 or less than −0.25.

tios. For sugar maple, either PCoA1 or PCoA2 was correlated with every C/nutrient ratio. In addition, for white ash, both PCoA1 and PCoA2 were correlated with all C/nutrient ratios except for some trace metals (Fe, Al, Cu, Mn). Notably, for white ash stakes, when mass loss was strongly negatively correlated with a C/nutrient ratio ($r < -0.75$), the C/nutrient ratio also showed similarly strong negative correlations with either fungal biomass, PCoA1, or PCoA2.

RDA revealed that sample points were more distinctly grouped by mass loss category (low, intermediate, high) when fungal community composition (PCoA1–2) (Figure 4a) was used as the predictor, compared to when fungal biomass was used (Figure 4b). For both wood species, grouping by mass loss was still apparent with biomass as the predictor, although the separation was less pronounced. When community composition was the predictor, B and Mg vectors had the largest association for sugar maple along RDA1, while Zn was the dominant nutrient along RDA2. For white ash, Ca, P, and Zn were the largest vectors along RDA1, with B explaining some variation along RDA2. In general, most nutrient vectors tended to associate with higher mass loss groups. When fungal biomass was the predictor, K was the largest vector for both wood species, largely explaining variance along RDA1. Proportion of variance explained (PVE) by accumulated constrained axes (RDA1, RDA2) is outlined in Supplemental Table B.

Results of the PCoA, paired with those of the cluster analysis, highlighted the distinct clustering of stakes by genetic dissimilarity (Figure 5a) and mass loss category (Figure 5b). Clustering was defined by PCoA axes and revealed three well-separated groups, indicating that the clusters were taxonomically structured. These clusters were further evaluated for mass loss differences and displayed significant variation in mass loss among the three groups (based on ANOVA; $p < 0.05$). For

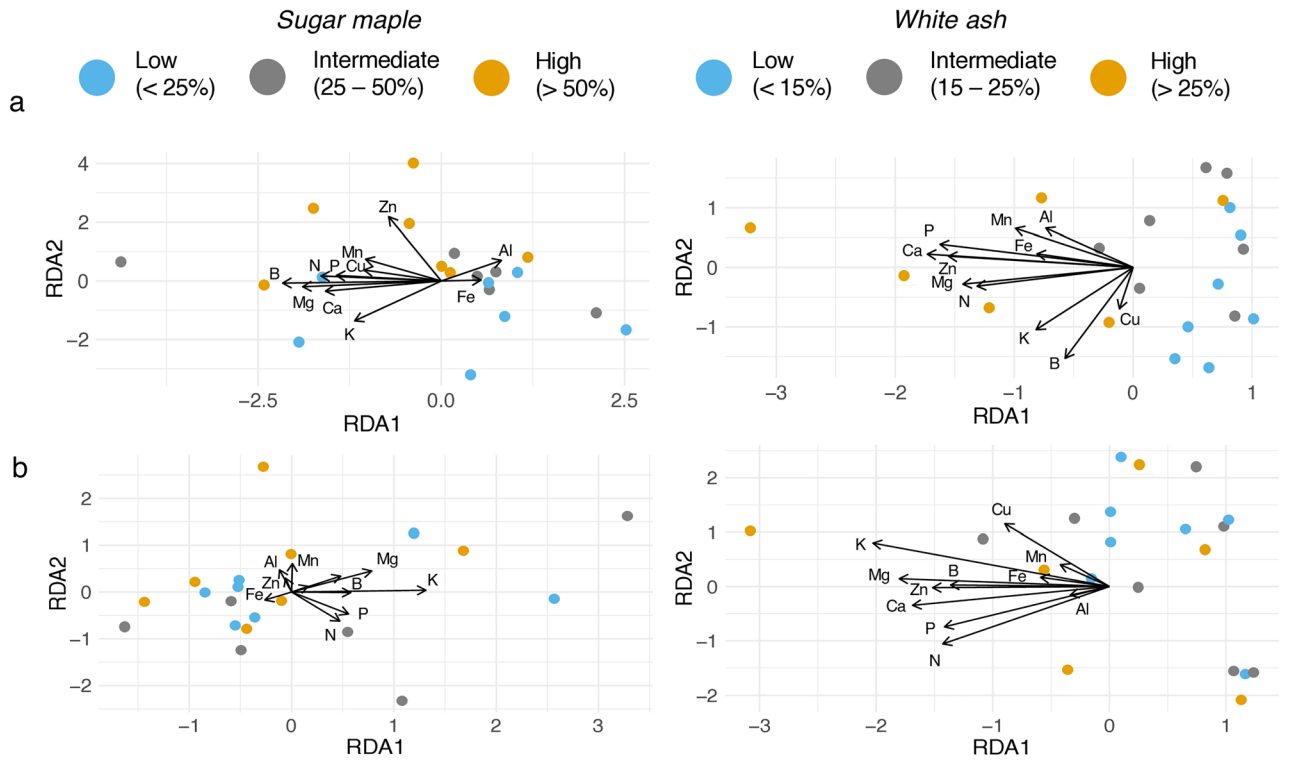

Figure 4. Redundancy Analysis (RDA) biplot showing the relationship between fraction of initial nutrient remaining (responses) and similarity in fungal community composition (**a**, top panels) and fungal biomass (**b**, bottom panels) as predictors (RDA1 and RDA2) for each species of wood. Points represent individual samples colored by mass loss category (low, intermediate, high), while arrows indicate the direction and strength of nutrient X/X_0 associations with the RDA axes. Arrows are scaled for visual clarity. Note that sample points are more distinctly grouped in the top panels, which include fungal community composition as the predictor, than in the bottom panels, which include fungal biomass as the predictor.

sugar maple samples, cluster 1 was dominated by *P. laevis*, cluster 2 by *S. fimbriatum*, and cluster 3 by *C. occidentalis*. For white ash, cluster 1 was dominated by *P. laevis*, cluster 2 by *P. lenta*, and cluster 3 by *Scopuloides hypnoides*. Clustering did not show a comparable pattern in fungal biomass, as fungal biomass did not differ significantly among cluster groups, with the exception of cluster 1 for white ash (Figure 5c). Consistent with our other results, clustering showed no statistical differences in C/nutrient ratios between groups for sugar maple, while high-mass-loss groups were different from low-mass-loss groups for white ash in many C/nutrient ratios (N, P, Ca, Mg, Fe, Mn, Zn, and B) (Supplemental Figure D).

Discussion

This study demonstrates that wood decomposition is jointly associated with fungal community composition, fungal biomass, and wood species identity. We found large variability in decomposition rates, with mass loss ranging from 8.6 to 94.7% for sugar maple stakes, and 4.1–35.8% for white ash. Sugar maple stakes showed greater mass loss than white ash stakes, potentially reflecting differences in wood chemistry and structure between diffuse-porous maple and ring-porous ash (Edelmann and others 2023; Forrester and others 2023).

Fungal community composition, as summarized by PCoA, was a significant statistical predictor of mass loss across top-performing linear regressions for both wood species, confirming its association with decomposition rates previously reported (Lindner and others 2011; Allison and others 2013; van der Wal and others 2015). For the highly variable sugar maple stakes, most variation in mass loss was explained by a single dominant pattern of fungal community composition (PCoA1), with fungal biomass contributing little additional explanatory power. In white ash, variation in mass loss was explained by a combination of fungal community composition (PCoA1 and PCoA2) and fungal biomass, indicating that multiple aspects of

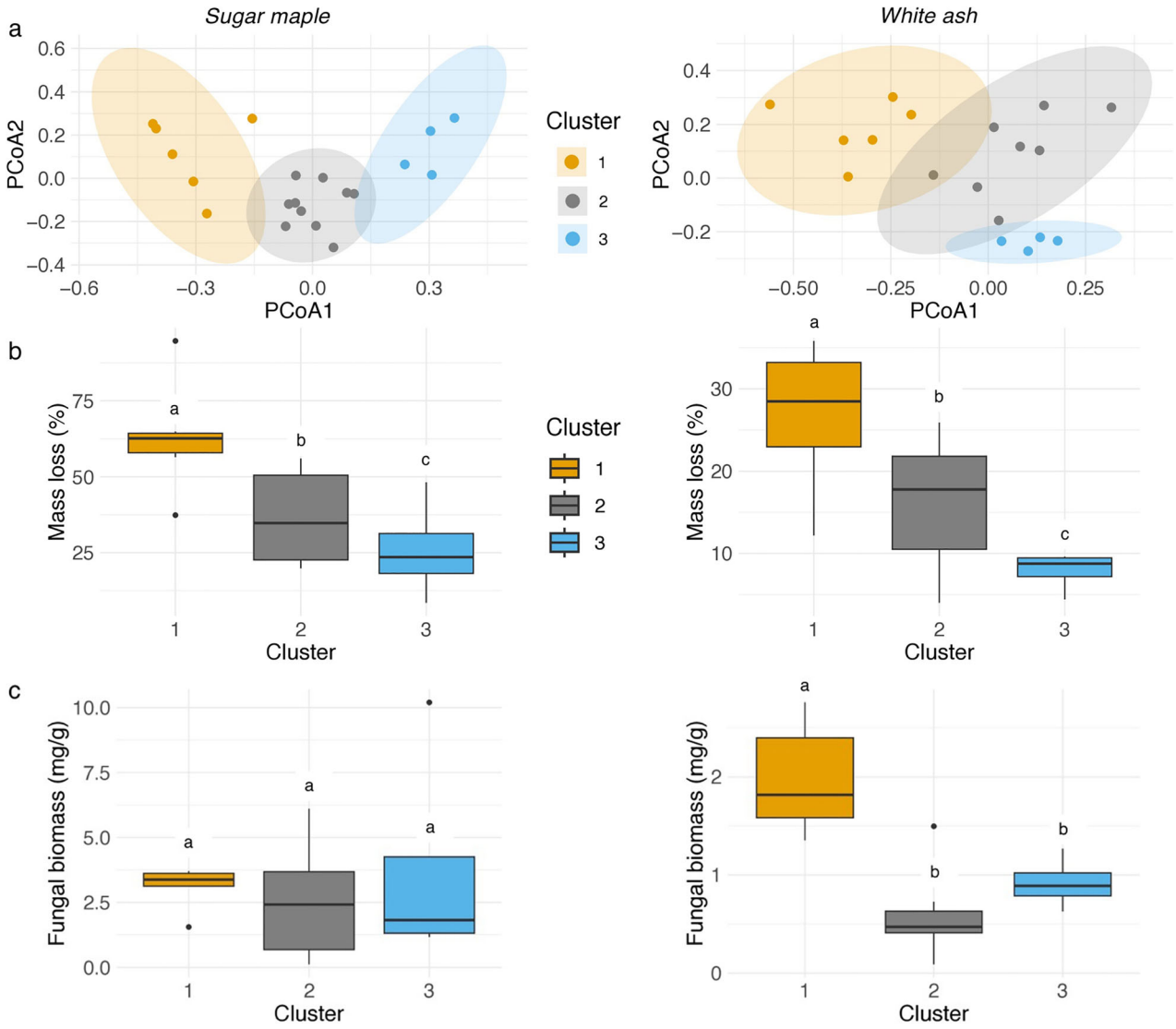

Figure 5. (**a**) Principal coordinate analysis (PCoA) showing fungal community clustering based on UniFrac distances. (**b**) Mass loss (%) across the three identified clusters. Colors correspond to clusters in both panels, with ellipses showing 95% confidence. Compact letter display shows difference among groups based on one-way ANOVA. (c) Fungal biomass (mg fungus/g wood) for each cluster.

fungal communities contribute to decomposition in this substrate.

However, the specific PCoA axis associated with mass loss differed by wood species, suggesting that distinct aspects of community composition were correlated with decomposition in sugar maple versus white ash. For maple, PCoA1 captured the primary gradient linked to rapid decay, whereas in ash, PCoA2 explained the greatest variation. Furthermore, the influence of fungal biomass varied by wood species, suggesting that some guilds accelerate decomposition presumably through higher abundance, whereas other, potentially more aggressive decomposers can accomplish rapid decay even at low biomass (Lustenhouwer and others 2020; Yang and others 2024). Alternatively, for white ash, which decomposed more slowly, the positive relationship between mass loss and fungal biomass may indicate that these stakes were in an active mid-decay phase, whereas many sugar maple stakes may have already progressed beyond this stage. These species-specific patterns suggest that host wood chemistry and structure filter fungal communities in ways that shape decomposition outcomes (Pánek and others 2024; Xu and others 2025).

Additional analyses provided independent support for the central role of fungal community

composition in explaining variation in mass loss. RDA revealed that samples grouped by mass loss when ordinated by community composition, whereas grouping was weaker under the fungal biomass predictor. In other words, low-fungal-biomass communities consisting of efficient decomposers could be associated with fast decomposition rates, whereas high-fungal-biomass communities dominated by less efficient taxa may not accelerate mass loss (Veen and others 2019). Alternatively, given that the fungal communities within stakes were at different successional states at the time of collection, which is very likely given the high variability in mass loss, the fungal metrics at collection may not capture the cumulative decomposition process. DNA sequencing and quantifying ergosterol at many points through time could elucidate successional mechanisms.

The cluster analyses further confirmed that fungal communities were associated with decomposition outcomes. Three distinct clusters, identified by genetic dissimilarity, corresponded to significantly different levels of mass loss. Notably, the dominant species characterizing each cluster were consistent with their known decay strategies. In sugar maple, the low-mass-loss cluster was dominated by *S. fimbriatum*, a white-rot typically associated with slower lignin degradation, while the high-mass-loss cluster was dominated by *P. laevis*, a white-rot fungus known for rapid decomposition of hardwood substrates. For white ash, the low-mass-loss cluster was dominated by *S. hypnoides*, a slower surface-level decomposer, and the high-mass-loss cluster again by *P. laevis*. These patterns demonstrate that the genetic structure of fungal communities aligns with functional differences in decomposition, suggesting that dominance by fungi with high ligninolytic potential is associated with higher hardwood mass loss rates across wood species (van der Wal and others 2015; Perreault and others 2023).

Because fungal community composition was a significant statistical predictor of mass loss, and nutrient concentrations and stoichiometry change as wood decays, we next explored how variation in fungal community composition and biomass covaried with nutrient patterns during decomposition. As expected, C/nutrient ratios were negatively correlated with mass loss. This pattern was observed for all nutrients except K, which exhibited a distinct behavior likely attributable to its high susceptibility to leaching (Arthur and Fahey 1990; Brown and others 1996; Krankina and others 1999). The consistently stronger correlations of PCoA axes, compared to those of fungal biomass (except N and P), with C/nutrient ratios and X/X_0 in sugar maple stakes confirm the findings of our regression analysis: Community composition was the primary variable associated with decomposition. Conversely, white ash stakes showed consistent correlations of both PCoA axes and fungal biomass with C/nutrient ratios, in agreement with white ash linear regression analysis. While this finding reinforces the notion that fungal biomass is coupled to nutrient supply (Gulis and others 2004, 2017), the set of broader correlations suggests that wood species-specific nutrient environments are related to fungal growth allocation.

In agreement with other studies (Johnson and others 2014), white ash stakes generally exhibited higher C/nutrient ratios in low-mass-loss clusters compared to high-mass-loss ones. In further exploring nutrient–decay relationships, the RDA indicated associations of obvious nutrients (N, P, Ca, Mg) with ordination gradients. More interestingly, B and Zn were strongly associated with ordination gradients, aligning with taxa characterized by low mass loss. This finding reinforces previous observations of the importance of Zn in fungal community function, with higher X/X_0 associated with faster lignin decomposers (Singhal and Rathore 2001; Di and others 2022). While B-related mechanisms remain largely unclear (Estevez-Fregoso and others 2021), our observation of relatively higher final B (and lower C:B) associated with faster decomposers warrants further ecological evaluation.

Additionally, higher X/X_0 was observed for several nutrients, namely Mn and Cu, in white ash compared to sugar maple. This finding paired with the positive correlation between mass loss and X/X_0 suggests greater immobilization of these nutrients during ash decay (values exceeding 1 indicate net accumulation). A possible explanation is that white ash may support taxa (such as members of the *Pholiota* lineage) more associated with early lignin modification (e.g., Mn-peroxidase and laccase activity), leading to slower but more consistent decomposition and tighter retention of Mn and Cu over the same period (Sack and others 1997). Alternatively, given the low nutrient concentrations in the wood and the relatively higher mass loss in sugar maple stakes, single timepoint sampling in this study may have captured the immobilization phase for white ash samples and the nutrient release phase for maple (Parton and others 2007). Further studies that evaluate changes in lignocellulose alongside community-level enzymatic and taxonomic markers are required to clarify these mechanisms.

Collectively, this study demonstrated that wood decomposition is jointly associated with fungal community composition, fungal biomass, and host wood identity. Across wood species, fungal community composition emerged as an important statistical predictor of mass loss linked to nutrient stoichiometry outcomes, whereas the influence of fungal biomass was only evident in white ash. Given the threatened extirpation of this species by the introduced emerald ash borer, our findings suggest loss of white ash may change the nature of future decomposition dynamics in these ecosystems (Herms and McCullough 2014). However, more data from multi-site replication, wood-trait characterization, and time-series sampling are required to properly evaluate these effects. Furthermore, taxonomically distinct fungal communities corresponded to functionally distinct decomposition outcomes, with dominant species' decay strategies likely aligning with mass loss patterns. Notably, fungal communities dominated by low biomass but efficient taxa could achieve rapid decay, whereas high-biomass communities dominated by less efficient taxa may not accelerate mass loss. However, given our single endpoint experimental design, further analyses across time-series are required to address mechanisms associated with successional dynamics, as well as efficiency metrics, of wood decomposers. Together, these results underscore the importance of fungal community dynamics and nutrient turnover in wood decomposition. Future studies of wood decomposition would benefit from time-series DNA-based characterization of fungal communities in wood tissue, particularly for tracking community shifts and colonization dynamics across time-series samples and decay stages.

Limitations

A key limitation of this study is its reliance on a single endpoint measurement after four years of decay, which constrains our ability to resolve successional dynamics in fungal communities and their temporal coupling to decomposition processes. For this reason, our goal was to provide descriptive, not causal, analyses at this endpoint. Because sequencing, fungal biomass, nutrient concentrations, and mass loss were only assessed at the final endpoint, the observed relationships likely integrate multiple, potentially distinct stages of decay, making it difficult to disentangle cause–effect relationships or identify transient community shifts. While ITS sequencing provides a useful snapshot of community composition, capturing DNA from both active and inactive (or dead) fungal taxa, it cannot resolve temporal turnover or distinguish taxa actively contributing to decomposition at earlier stages.

Time-series sampling would allow for more direct tracking of fungal colonization, succession, and functional transitions and would better link community composition and biomass to nutrient dynamics and decomposition rates. Additionally, we did not quantify decomposer efficiency (e.g., carbon use efficiency (CUE)), limiting our ability to determine if rapid decay reflects greater biomass accumulation or higher per-unit activity of dominant taxa. Incorporating such efficiency metrics alongside repeated measurements through time would provide a more mechanistic understanding of how fungal communities regulate wood decomposition. Further limitations include the single-site design, which may constrain the generalizability of these findings to other forest systems with differing climate, soil conditions, and species pools, as well as the lack of plot-level microclimate measurements, which precludes any assessment of how moisture and temperature influence decomposition rates. Moreover, ergosterol provides only a coarse proxy for fungal biomass (e.g., varying across taxa and potentially decoupled from activity), and PCoA axes represent composite statistical gradients that may not map cleanly onto specific ecological processes, limiting mechanistic interpretation of community–function relationships.

ACKNOWLEDGEMENTS

This research was supported in part by the Maine Agricultural and Forest Experiment Station (ME042612) and the University of Maine Analytical Laboratory. We thank Paulina Murray, Logan Quinn, and Ethan Charles for their contributions, as well as Dartmouth College Woodlands for access to the study areas used for this work. We thank the editors and reviewers for their constructive feedback, which improved the clarity of the manuscript.

DATA AVAILABILITY

The data generated and used in this study are available on the Environmental Data Initiative (EDI) repository (Hettwer and others 2026) at: https://portal.edirepository.org/nis/mapbrowse?packageid=edi.2373.1.

Declarations

Conflict of interest The authors have no conflicts of interest to report.

OPEN ACCESS

REFERENCES

Abarenkov K, Nilsson RH, Larsson K-H, Taylor AFS, May TW, Frøslev TG, Pawlowska J, Lindahl B, Põldmaa K, Truong C, Vu D, Hosoya T, Niskanen T, Piirmann T, Ivanov F, Zirk A, Peterson M, Cheeke TE, Ishigami Y, Jansson AT, Jeppesen TS, Kristiansson E, Mikryukov V, Miller JT, Oono R, Ossandon FJ, Paupério J, Saar I, Schigel D, Suija A, Tedersoo L, Kõljalg U. 2024. The UNITE database for molecular identification and taxonomic communication of fungi and other eukaryotes: sequences, taxa and classifications reconsidered. Nucleic Acids Research 52:D791–D797. https://doi.org/10.1093/nar/gkad1039.Lastaccessed10/12/2025.

Allison SD, Lu Y, Weihe C, Goulden ML, Martiny AC, Treseder KK, Martiny JBH. 2013. Microbial abundance and composition influence litter decomposition response to environmental change. Ecology 94:714–725. https://doi.org/10.1890/12-1243.1.

Arthur MA, Fahey TJ. 1990. Mass and nutrient content of decaying boles in an Engelmann spruce – subalpine fir forest, Rocky Mountain National Park, Colorado. Canadian Journal of Forest Research 20:730–7. https://cdnsciencepub.com/doi/abs/https://doi.org/10.1139/x90-096. Last accessed 06/01/2026

Avis PG, Goldman LL, Carrara JE, Fernandez I. 2025. Six years later: Ectomycorrhizal fungal communities recovering after the end of long-term nitrogen and sulfur addition in a mixed-species temperate North American forest. Fungal Ecology 76:101436–101436. https://www.sciencedirect.com/science/article/pii/S1754504825000261

Baldrian P, Větrovský T, Cajthaml T, Dobiášová P, Petránková M, Šnajdr J, Eichlerová I. 2013. Estimation of fungal biomass in forest litter and soil. Fungal Ecology 6:1–11. https://www.sciencedirect.com/science/article/pii/S1754504812001274. Last accessed 10/12/2025

Boddy L. 2001. Fungal Community Ecology and Wood Decomposition Processes in Angiosperms: From Standing Tree to Complete Decay of Coarse Woody Debris. Ecological Bulletins 49:43–56.

Boddy L, Watkinson SC. 1995. Wood decomposition, higher fungi, and their role in nutrient redistribution. Canadian Journal of Botany 73:1377–83. https://cdnsciencepub.com/doi/https://doi.org/10.1139/b95-400. Last accessed 08/01/2026

Bradford MA, Warren RJ, Baldrian P, Crowther TW, Maynard DS, Oldfield EE, Wieder WR, Wood SA, King JR. 2014. Climate fails to predict wood decomposition at regional scales. Nature Climate Change 4:625–630.

Brown S, Mo J, McPherson JK, Bell DT. 1996. Decomposition of woody debris in Western Australian forests. Canadian Journal of Forest Research 26:954–66. https://cdnsciencepub.com/doi/https://doi.org/10.1139/x26-105. Last accessed 06/01/2026

Buness V, Gundale MJ, Lindahl BD, Gangiah TK, Annighöfer P, Josefsson T, Wieser NI, Metcalfe DB, Lanzrein I, Ali ST, Nilsson M-C, Sundqvist MK. 2026. Distinct diversity trajectories of boreal wood-inhabiting fungi following fire versus clear-cutting. Journal of Ecology 114:e70296. https://onlinelibrary.wiley.com/doi/abs/https://doi.org/10.1111/1365-2745.70296. Last accessed 24/04/2026

Craine J, Morrow C, Fierer N. 2007. Microbial nitrogen limitation increase decomposition. Ecology 88:2105–2113.

Dalling JW, Flores III MR, Heineman KD. 2024. Wood nutrients: Underexplored traits with functional and biogeochemical consequences. New Phytologist 244:1694–708. https://onlinelibrary.wiley.com/doi/abs/https://doi.org/10.1111/nph.20193. Last accessed 05/01/2026

Di W, Yuying M, Teng Y, Guifeng G, Daozhong W, Xisheng G, Haiyan C. 2022. Phosphorus and Zinc Are Strongly Associated with Belowground Fungal Communities in Wheat Field under Long-Term Fertilization. Microbiology Spectrum 10:e00110-e122. https://doi.org/10.1128/spectrum.00110-22.

Edelmann P, Weisser WW, Ambarlı D, Bässler C, Buscot F, Hofrichter M, Hoppe B, Kellner H, Minnich C, Moll J, Persoh D, Seibold S, Seilwinder C, Schulze E-D, Wöllauer S, Borken W. 2023. Regional variation in deadwood decay of 13 tree species: Effects of climate, soil and forest structure. Forest Ecology and Management 541:121094. https://www.sciencedirect.com/science/article/pii/S0378112723003286. Last accessed 05/05/2026

Estevez-Fregoso E, Farfán-García ED, García-Coronel IH, Martínez-Herrera E, Alatorre A, Scorei RI, Soriano-Ursúa MA. 2021. Effects of boron-containing compounds in the fungal kingdom. Journal of Trace Elements in Medicine and Biology 65:126714. https://www.sciencedirect.com/science/article/pii/S0946672X21000043. Last accessed 28/04/2026

Forrester JA, Fraver S, Mladenoff DJ, Gower ST, D'Amato AW, Lindner DL. 2023. Experimental Evidence that Forest Structure Controls Detrital Decomposition. Ecosystems 26:1396–1410. https://doi.org/10.1007/s10021-023-00841-5.Lastaccessed10/12/2025.

Fukami T, Dickie IA, Paula Wilkie J, Paulus BC, Park D, Roberts A, Buchanan PK, Allen RB. 2010. Assembly history dictates ecosystem functioning: evidence from wood decomposer communities. Ecology Letters 13:675–684. https://doi.org/10.1111/j.1461-0248.2010.01465.x.

Fukasawa Y. 2021. Ecological impacts of fungal wood decay types: A review of current knowledge and future research

directions. Ecological Research 36:910–931. https://doi.org/10.1111/1440-1703.12260.

Gulis V, Kuehn KA, Schoettle LN, Leach D, Benstead JP, Rosemond AD. 2017. Changes in nutrient stoichiometry, elemental homeostasis and growth rate of aquatic litter-associated fungi in response to inorganic nutrient supply. The ISME Journal 11:2729–2739. https://doi.org/10.1038/ismej.2017.123.

Gulis V, Rosemond AD, Suberkropp K, Weyers HS, Benstead JP. 2004. Effects of nutrient enrichment on the decomposition of wood and associated microbial activity in streams. Freshwater Biology 49:1437–1447. https://doi.org/10.1111/j.1365-2427.2004.01281.x.

Harmon ME, Franklin JF, Swanson FJ, Sollins P, Gregory SV, Lattin JD, Anderson NH, Cline SP, Aumen NG, Sedell JR, Lienkaemper GW, Cromack K, Cummins KW. 1986. Ecology of Coarse Woody Debris in Temperate Ecosystems. In: MacFadyen A, Ford ED, editors. Advances in Ecological Research. Vol. 15. Academic Press. pp 133–302. https://www.sciencedirect.com/science/article/pii/S006525040860121X

Harmon ME, Sexton J, Caldwell BE, Carpenter SE. 1994. Fungal sporocarp mediated losses of Ca, Fe, K, Mg, Mn, N, P, and Zn from conifer logs in the early stages of decomposition.

Herms DA, McCullough DG. 2014. Emerald Ash Borer Invasion of North America: History, Biology, Ecology, Impacts, and Management. Annual Review of Entomology 59:13–30. https://doi.org/10.1146/annurev-ento-011613-162051.

Hettwer C, Fraver S, Ouimette A, Bosley-Smith C, D'Amato A, Avis P. 2026. Geochemical analysis of Fraxinus americana and Acer saccharum wood after four years of decomposition in a northern temperate deciduous forest, Corinth, VT USA, 2024 ver 1. Environmental Data Initiative. Accessed 2026-06-02. https://doi.org/10.6073/pasta/edd1084c7eed06294efa1e0ce92e1ed2.

Hobbie S, Vitousek P. 2000. Nutrient Limitation of Decomposition in Hawaiian Forests. Ecology 81:1867–1877.

Holub SM, Spears JDH, Lajtha K. 2001. A reanalysis of nutrient dynamics in coniferous coarse woody debris. Canadian Journal of Forest Research 31:1894–1902.

Johnson CE, Siccama TG, Denny EG, Koppers MM, Vogt DJ. 2014. In situ decomposition of northern hardwood tree boles: Decay rates and nutrient dynamics in wood and bark. Canadian Journal of Forest Research 44:1515–1524.

Klockow P, D'Amato A, Bradford J, Fraver S. 2014. Nutrient concentrations in coarse and fine woody debris of Populus tremuloides Michx.-dominated forests, Northern Minnesota, USA. Silva Fennica 48.

Koide RT, Malcolm GM. 2009. N concentration controls decomposition rates of different strains of ectomycorrhizal fungi. Fungal Ecology 2:197–202. https://linkinghub.elsevier.com/retrieve/pii/S1754504809000658. Last accessed 10/12/2025

Krankina ON, Harmon ME, Griazkin AV. 1999. Nutrient stores and dynamics of woody detritus in a boreal forest: modeling potential implications at the stand level. Canadian Journal of Forest Research 29:20–32. https://cdnsciencepub.com/doi/abs/https://doi.org/10.1139/x98-162. Last accessed 06/01/2026

Krzesłowska M, Mleczek P, Budka A, Siwulski M, Budzyńska S, Niedzielski P, Árvay J, Mleczek M. 2025. Elemental uptake and accumulation by wood decay fungi in relation to their nutrition strategy, rot type and mineral profile of the colonized wood. Fungal Biology 129:101592. https://www.sciencedirect.com/science/article/pii/S1878614625000583. Last accessed 29/04/2026

Kubartová A, Ottosson E, Stenlid J. 2015. Linking fungal communities to wood density loss after 12 years of log decay. FEMS Microbiology Ecology 91:fiv032. https://doi.org/10.1093/femsec/fiv032. Last accessed 24/04/2026

Laiho R, Prescott CE. 1999. The contribution of coarse woody debris to carbon, nitrogen, and phosphorus cycles in three Rocky Mountain coniferous forests. Canadian Journal of Forest Research 29:1592–603. https://cdnsciencepub.com/doi/https://doi.org/10.1139/x99-132. Last accessed 10/12/2025

Laiho R, Prescott CE. 2004. Decay and nutrient dynamics of coarse woody debris in northern coniferous forests: a synthesis. Canadian Journal of Forest Research 34:763–77. https://cdnsciencepub.com/doi/https://doi.org/10.1139/x03-241. Last accessed 10/12/2025

Lauber CL, Zhou N, Gordon JI, Knight R, Fierer N. 2010. Effect of storage conditions on the assessment of bacterial community structure in soil and human-associated samples. FEMS Microbiology Letters 307:80–86.

Legge EOL, Fitch A, Goldsmith S, D'Amato AW, Evans K, Hicks Pries CE. 2025. Negative effects of belowground competition outweigh potential benefits of arbuscular mycorrhizal facilitation for seedling success in a managed temperate hardwood forest. Canadian Journal of Forest Research 55:1–14. https://cdnsciencepub.com/doi/https://doi.org/10.1139/cjfr-2024-0259. Last accessed 10/12/2025

Lindner DL, Vasaitis R, Kubartová A, Allmér J, Johannesson H, Banik MT, Stenlid J. 2011. Initial fungal colonizer affects mass loss and fungal community development in Picea abies logs 6yr after inoculation. Fungal Ecology 4:449–60. https://www.sciencedirect.com/science/article/pii/S1754504811000717

Lustenhouwer N, Maynard DS, Bradford MA, Lindner DL, Oberle B, Zanne AE, Crowther TW. 2020. A trait-based understanding of wood decomposition by fungi. Proceedings of the National Academy of Sciences 117:11551–11558. https://doi.org/10.1073/pnas.1909166117.

Manzoni S, Trofymow JA, Jackson RB, Porporato A. 2010. Stoichiometric controls on carbon, nitrogen, and phosphorus dynamics in decomposing litter. Ecological Monographs 80:89–106. https://doi.org/10.1890/09-0179.1.

Maynard DS, Covey KR, Crowther TW, Sokol NW, Morrison EW, Frey SD, van Diepen LTA, Bradford MA. 2018. Species associations overwhelm abiotic conditions to dictate the structure and function of wood-decay fungal communities. Ecology 99:801–11. https://onlinelibrary.wiley.com/doi/abs/https://doi.org/10.1002/ecy.2165. Last accessed 07/04/2026

McMurdie PJ, Holmes S. 2013. phyloseq: An R Package for Reproducible Interactive Analysis and Graphics of Microbiome Census Data. PLOS ONE 8:e61217. https://journals.plos.org/plosone/article?id=https://doi.org/10.1371/journal.pone.0061217. Last accessed 10/12/2025

Micó E, Aguirrebengoa M, Quinto J, Juárez M, Marmaneu J, Sánchez A. 2024. Physical decomposition stage and ergosterol content predict the chemical composition of downed dead wood in Mediterranean dehesas. European Journal of Forest Research 143:1117–1133. https://doi.org/10.1007/s10342-024-01672-2.

Morvan S, Meglouli H, Lounès-Hadj Sahraoui A, Hijri M. 2020. Into the wild blueberry (Vaccinium angustifolium) rhizosphere microbiota. Environmental Microbiology 22:3803–3822. https://doi.org/10.1111/1462-2920.15151.

Newell SY, Arsuffi TL, Fallon2 ARD. 1988. Fundamental Procedures for Determining Ergosterol Content of Decaying Plant Material by Liquid Chromatography.

Oksanen J, Simpson GL, Blanchet FG, Kindt R, Legendre P, Minchin PR, O'Hara RB, Solymos P, Stevens MHH, Szoecs E, Wagner H, Barbour M, Bedward M, Bolker B, Borcard D, Borman T, Carvalho G, Chirico M, De Caceres M, Durand S, Evangelista HBA, FitzJohn R, Friendly M, Furneaux B, Hannigan G, Hill MO, Lahti L, Martino C, McGlinn D, Ouellette M-H, Ribeiro Cunha E, Smith T, Stier A, Ter Braak CJF, Weedon J. 2025. vegan: Community Ecology Package. :2.7–2. https://CRAN.R-project.org/package=vegan. Last accessed 10/12/2025

Pan Y, Birdsey RA, Fang J, Houghton R, Kauppi PE, Kurz WA, Phillips OL, Shvidenko A, Lewis SL, Canadell JG, Ciais P, Jackson RB, Pacala SW, McGuire A, Piao S, Rautiainen A, Sitch S, Hayes D. 2011. A large and persistent carbon sink in the world's forests. Science 333:988–93. https://pubs.usgs.gov/publication/70034599

Pánek M, Vlková T, Michalová T, Borovička J, Tedersoo L, Adamczyk B, Baldrian P, Lopéz-Mondéjar R. 2024. Variation of carbon, nitrogen and phosphorus content in fungi reflects their ecology and phylogeny. Frontiers in Microbiology Volume 15–2024. https://www.frontiersin.org/journals/microbiology/articles/https://doi.org/10.3389/fmicb.2024.1379825

Paradis E, Claude J, Strimmer K. 2004. APE: Analyses of Phylogenetics and Evolution in R language. Bioinformatics 20:289–290. https://doi.org/10.1093/bioinformatics/btg412.

Parton W, Silver WL, Burke IC, Grassens L, Harmon ME, Currie WS, King JY, Adair EC, Brandt LA, Hart SC, Fasth B. 2007. Global-Scale Similarities in Nitrogen Release Patterns During Long-Term Decomposition. Science 315:361–4. https://www.science.org/doi/https://doi.org/10.1126/science.1134853. Last accessed 02/06/2026

Perreault L, Forrester JA, Lindner DL, Jusino MA, Fraver S, Banik MT, Mladenoff DJ. 2023. Linking wood-decay fungal communities to decay rates: Using a long-term experimental manipulation of deadwood and canopy gaps. Fungal Ecology 62:101220–101220. https://www.sciencedirect.com/science/article/pii/S1754504822000812

Pinheiro J, Bates D, R Core Team. 2025. nlme: Linear and Nonlinear Mixed Effects Models. https://svn.r-project.org/R-packages/trunk/nlme/. Last accessed 10/12/2025

Posit Team. 2025. RStudio: Integrated Development Environment for R. https://posit.co/. Last accessed 10/12/2025

PRISM Group. 2024. PRISM Group at Oregon State University. https://prism.oregonstate.edu/. Last accessed 10/12/2025

Purahong W, Hoppe B, Kahl T, Schloter M, Schulze E-D, Bauhus J, Buscot F, Krüger D. 2014. Changes within a single land-use category alter microbial diversity and community structure: Molecular evidence from wood-inhabiting fungi in forest ecosystems. Journal of Environmental Management 139:109–19. https://www.sciencedirect.com/science/article/pii/S0301479714001224

Purahong W, Wubet T, Lentendu G, Hoppe B, Jariyavidyanont K, Arnstadt T, Baber K, Otto P, Kellner H, Hofrichter M, Bauhus J, Weisser WW, Krüger D, Schulze E-D, Kahl T, Buscot F. 2018. Determinants of Deadwood-Inhabiting Fungal Communities in Temperate Forests: Molecular Evidence From a Large Scale Deadwood Decomposition Experiment. Frontiers in Microbiology Volume 9–2018. https://www.frontiersin.org/journals/microbiology/articles/https://doi.org/10.3389/fmicb.2018.02120

R Core Team. 2025. R: A language and environment for statistical computing. https://www.R-project.org/. Last accessed 10/12/2025

Romero LM, Smith TJ, Fourqurean JW. 2005. Changes in mass and nutrient content of wood during decomposition in a south Florida mangrove forest. Journal of Ecology 93:618–631.

Runnel K, Drenkhan R, Adamson K, Lõhmus P, Rosenvald K, Rosenvald R, Rähn E, Tedersoo L. 2021. The factors and scales shaping fungal assemblages in fallen spruce trunks: A DNA metabarcoding study. Forest Ecology and Management 495:119381–119381. https://www.sciencedirect.com/science/article/pii/S0378112721004692

Sack U, Hofrichter M, Fritsche W. 1997. Degradation of polycyclic aromatic hydrocarbons by manganese peroxidase of Nematoloma frowardii. FEMS Microbiology Letters 152:227–234. https://doi.org/10.1111/j.1574-6968.1997.tb10432.x.Lastaccessed05/05/2026.

Schilling JS, Kaffenberger JT, Held BW, Ortiz R, Blanchette RA. 2020. Using Wood Rot Phenotypes to Illuminate the ''Gray'' Among Decomposer Fungi. Frontiers in Microbiology 11:1288. https://pmc.ncbi.nlm.nih.gov/articles/PMC7303305/. Last accessed 07/04/2026

Schmidt O, editor. 2006. Wood Rot. In: Wood and Tree Fungi: Biology, Damage, Protection, and Use. Berlin, Heidelberg: Springer. pp 135–59. https://doi.org/10.1007/3-540-32139-X_7. Last accessed 10/12/2025

Seibold S, Müller J, Allner S, Willner M, Baldrian P, Ulyshen MD, Brandl R, Bässler C, Hagge J, Mitesser O. 2022. Quantifying wood decomposition by insects and fungi using computed tomography scanning and machine learning. Scientific Reports 12:16150–16150. https://doi.org/10.1038/s41598-022-20377-3.

Singhal V, Rathore VS. 2001. Effects of Zn2+ and Cu2+ on growth, lignin degradation and ligninolytic enzymes in Phanerochaete chrysosporium. World Journal of Microbiology and Biotechnology 17:235–240. https://doi.org/10.1023/A:1016617025769.

Sterner R, Elser JJ. 2002. Ecological Stoichiometry: The Biology of Elements From Molecules to The Biosphere. pp 439–439.

Toju H, Tanabe AS, Yamamoto S, Sato H. 2012. High-Coverage ITS Primers for the DNA-Based Identification of Ascomycetes and Basidiomycetes in Environmental Samples. PLOS ONE 7:e40863. https://doi.org/10.1371/journal.pone.0040863.

Veen GF (Ciska), Snoek BL, Bakx-Schotman T, Wardle DA, van der Putten WH. 2019. Relationships between fungal community composition in decomposing leaf litter and home-field advantage effects. Functional Ecology 33:1524–35. https://doi.org/10.1111/1365-2435.13351

Viotti C, Bach C, Maillard F, Ziegler-Devin I, Mieszkin S, Buée M. 2021. Sapwood and heartwood affect differentially bacterial and fungal community structure and successional dynamics during Quercus petraea decomposition. Environmental Microbiology 23:6177–93. https://onlinelibrary.wiley.com/doi/abs/https://doi.org/10.1111/1462-2920.15522. Last accessed 07/04/2026

van der Wal A, Ottosson E, de Boer W. 2015. Neglected role of fungal community composition in explaining variation in wood decay rates. Ecology 96:124–133. https://doi.org/10.1890/14-0242.1.

Woodall CW, Heath LS, Smith JE. 2008. National inventories of down and dead woody material forest carbon stocks in the United States: Challenges and opportunities. Forest Ecology and Management 256:221–8. https://www.sciencedirect.com/science/article/pii/S0378112708003204

Wu C, Shu C, Zhang Z, Zhang Y, Liu Y. 2021. Phosphorus deposition accelerates wood decomposition and temperature sensitivity in a subtropical forest. Ecological Indicators 128:107819–107819. https://www.sciencedirect.com/science/article/pii/S1470160X21004842

Xu Z, Hu Z, Jiang L, Qiu T, Li W, Anthony MA. 2025. Contrasting wood carbon quality of angiosperms and gymnosperms drives fungal-mediated decomposition responses to nutrient enrichment. Forest Ecology and Management 593:122910–122910. https://www.sciencedirect.com/science/article/pii/S0378112725004189

Yang S, Poorter L, Sterck FJ, Cornelissen JHC, van Logtestijn RSP, Kuramae EE, Kowalchuk GA, Hefting MM, Goudzwaard L, Chang C, Sass-Klaassen U. 2024. Stem decomposition of temperate tree species is determined by stem traits and fungal community composition during early stem decay. Journal of Ecology 112:1240–1255. https://doi.org/10.1111/1365-2745.14295.